PHYSICAL REVIEW B VOLUME 48, NUMBER 12 15 SEPTEMBER 1993-II

Electronic properties and phase transitions of RbC_{60} and CsC_{60}: Investigation by NMR spectroscopy

R. Tycko, G. Dabbagh, and D. W. Murphy
AT&T Bell Laboratories, 600 Mountain Avenue, Murray Hill, New Jersey 07974

Q. Zhu and J. E. Fischer
Department of Materials Science and Engineering, University of Pennsylvania, Philadelphia, Pennsylvania 19104

(Received 18 March 1993)

We report the results of ^{133}Cs, ^{87}Rb, and ^{13}C NMR measurements on the alkali-metal fullerides CsC_{60} and RbC_{60}. Measurements of NMR spectra and spin-lattice relaxation rates provide clear evidence for phase transitions near 300 K in both compounds, with substantial changes in their electronic properties at the phase transitions. The high-temperature phases are paramagnets, with an exchange coupling of roughly 2 cm^{-1} between electron spins that are localized primarily on C_{60}^{-} ions. The ^{133}Cs and ^{87}Rb NMR frequency shifts and relaxation rates are determined by Fermi contact hyperfine couplings to the electron spins. The ^{13}C relaxation rates are determined by dipolar hyperfine couplings. The electron-spin susceptibility is greatly reduced in the low-temperature phases

I. INTRODUCTION

Since the first synthesis of alkali-metal fullerides A_xC_{60} (A =Na, K, Rb, Cs) by Haddon *et al.*,[1] a great deal of effort has been devoted to the characterization of the structural, electronic, and dynamic properties of these materials, both experimentally and theoretically. Much of the current interest in the alkali-metal fullerides stems from the discovery of superconductivity in A_3C_{60} compounds,[2-6] with superconducting transition temperatures (T_c) as high as 33 K. In general, alkali-metal fullerides are formed by intercalation of metal atoms into interstitial sites between C_{60} molecules in solid C_{60}. The alkali-metal atoms are almost fully ionized to A^+, donating electrons to the triply degenerate t_{1u} LUMO (lowest unoccupied molecular orbital) of C_{60} molecules. The LUMO is constructed primarily from carbon $2p_z$ orbitals, with some admixture of $2s$ character due to the molecule's curvature.[7] For A =K, Rb, or Cs, thermodynamically stable phases with $x=3$, 4, and 6 have been structurally characterized.[8-10] Of these, only the A_3C_{60} compounds, in which the electronic conduction band formed from overlapping C_{60} LUMO's is nominally half full, have been shown to be conductors and superconductors. The conduction-band widths of the A_3C_{60} compounds have been estimated to be 200–700 meV.[11-18] Conductivities are 10^{-2}–10^{-3} Ω cm.[19-21] The A_6C_{60} compounds, in which the conduction band is nominally full, are semiconductors. The A_4C_{60} compounds, with a partially filled conduction band, might be expected to be conductors, but the existing experimental data from conductivity measurements on thin films,[19,21] photoemission spectroscopy,[21] muon spin resonance,[22] and nuclear magnetic resonance (NMR) relaxation measurements[23] indicate that they are not. The nature of the electronic properties in A_4C_{60} compounds remains poorly understood.

Recently, the existence of a fourth stable phase of alkali-metal fullerides, with stiochiometry A_1C_{60} (A =K, Rb, Cs), has been demonstrated.[24-27] Zhu *et al.*[26] found evidence, based on differential scanning calorimetry (DSC) and x-ray powder diffraction (XRD) measurements, for structural phase transitions in these compounds in the temperature range from 300 to 450 K. At the highest temperatures studied, the A_1C_{60} compounds adopt a NaCl structure, in which the C_{60}^{-} ions have their centers of mass on a fcc lattice and the A^+ ions are located in the octahedrally coordinated sites between C_{60}^{-} ions. At the lowest temperatures, the structures are not cubic.

The nature of the electronic properties of the A_1C_{60} compounds, in both the high- and low-temperature phases, are largely unknown. Conductivity and photoemission measurements on K- and Rb-intercalated thin films of C_{60}, carried out as a function of nominal stoichiometry,[19,21] indicate that electrical conductors are formed only near $x=3$. At all other stoichiometries, semiconducting or insulating behavior is observed. On the other hand, as in the case of the A_4C_{60} compounds, the partially filled conduction band in the A_1C_{60} compounds suggests that they should be conductors in a single-electron model, in at least one of their structural phases.

In this paper, we present the results of ^{13}C, ^{87}Rb, and ^{133}Cs NMR measurements on RbC_{60} and CsC_{60}. Our measurements of the temperature dependence of the NMR spectra and nuclear-spin-lattice relaxation rates provide dramatic evidence for a structural phase transition near 300 K in both compounds, in agreement with XRD and DSC results.[26] Both the NMR frequencies and the relaxation rates change substantially at the transition, indicating a qualitative change in the electronic properties. Our NMR data for the high-temperature (HT) phases indicate that the HT phases are paramagnets. Unpaired electrons are principally localized on individual

0163-1829/93/48(12)/9097(9)/$06.00

C_{60}^{-} ions, with an exchange coupling of roughly 2 cm^{-1} between the localized electron spins. Thus electron-electron interactions dominate the electronic dynamics. This is in obvious contrast to the A_3C_{60} compounds, in which NMR and other data can be explained by a Fermi-liquid model in which electron-electron interactions play a relatively minor role.[11-16]

Our characterization of the low-temperature (LT) phases is less complete. Nonetheless, the NMR data show that the electron-spin susceptibility is greatly reduced in the LT phases, i.e., most unpaired electron spins in the HT phases apparently become paired in the LT phases.

II. EXPERIMENTAL METHODS

Samples of RbC_{60} and CsC_{60} powder were prepared as described previously.[3,28] Briefly, the corresponding A_6C_{60} compounds were formed by reaction of C_{60} powder with excess alkali-metal vapor in sealed pyrex tubes at 250–300 °C. A_6C_{60} was then diluted with the appropriate amount of C_{60} and annealed for several days at 300 °C (for RbC_{60}) or a week at 450–500 °C (for CsC_{60}). 58 mg of CsC_{60} and roughly 30 mg of RbC_{60} were used in the NMR measurements. Our CsC_{60} sample was prepared identically to those studied by DSC and XRD by Zhu *et al.*[26]

NMR measurements were carried out in a 9.39-T field, corresponding to ^{13}C NMR frequencies near 100.5 MHz, ^{87}Rb frequencies near 130.7 MHz, and ^{133}Cs frequencies near 52.4 MHz. The spin-lattice relaxation (SLR) data presented in Figs. 3 and 6 were obtained with the saturation-recovery technique. The recovery curves were fit to the single-exponential form $S(\tau)=S_0-S_1e^{-\tau/T_1}$, where $S(\tau)$ is the signal amplitude (peak height in the NMR spectrum) for a recovery time τ, and T_1 is the apparent relaxation time. In all cases, this form for $S(\tau)$ provided a good fit to the experimental data to within the experimental noise limits. In the case of quadrupolar nuclei (e.g., ^{87}Rb and ^{133}Cs), it is well known that the SLR kinetics may involve more than one time constant, depending on the details of the initial spin state prepared by the saturating radio-frequency (rf) pulses.[29] For magnetic relaxation, if all of the spin transitions are saturated by the rf pulses, as is the case when the rf Rabi frequency is much larger than the quadrupole coupling, then the recovery curves are single exponential. If only the central transition ($m=\frac{1}{2}\rightarrow m=-\frac{1}{2}$) is affected by the pulses, as is the case when the quadrupole coupling is much larger than the Rabi frequency, then the recovery curves have the form $S(\tau)=S_0-S_1(\frac{9}{10}e^{-6\tau/T_1}+\frac{1}{10}e^{-\tau/T_1})$ for a spin-$\frac{3}{2}$ nucleus (e.g., ^{87}Rb) and the form $S(\tau)=S_0-S_1(\frac{1225}{1716}e^{-28\tau/T_1}+\frac{75}{364}e^{-15\tau/T_1}+\frac{3}{44}e^{-6\tau/T_1}+\frac{1}{84}e^{-\tau/T_1})$ for a spin-$\frac{7}{2}$ nucleus (e.g., ^{133}Cs). In the ^{133}Cs NMR measurements leading to Fig. 3(a), the rf field amplitude B_1 was large enough to saturate all of the spin transitions ($B_1\approx 110$ G), as evidenced by the fact that the Rabi frequency for the ^{133}Cs signals from CsC_{60} was nearly the same as the Rabi frequency for the ^{133}Cs signals from a $CsCl_{(aq)}$ reference sample. The reported T_1 values are therefore quantitatively accurate representations of the relaxation kinetics. In the ^{87}Rb NMR measurements leading to Fig. 6(a), the rf fields were not large enough to saturate all of the spin transitions ($B_1\approx 60$ G). The reported T_1 values are therefore somewhat smaller than the true values that would be measured either with much stronger or much weaker rf fields. Inversion-recovery measurements were carried out on RbC_{60} at several temperatures using $B_1\approx 2$ G, and analyzed by fits to the form $S(\tau)=S_0-S_1(\frac{9}{10}e^{-6\tau/T_1}+\frac{1}{10}e^{-\tau/T_1})$ appropriate for selective excitation of the central transition. The T_1 values determined from these selective excitation measurements were roughly 30% larger than those reported in Fig. 6(a).

We observed significant hysteresis in the phase transitions described below, as noted by Zhu *et al.*,[26] particularly in CsC_{60}. Care was taken to ensure that the NMR spectra and relaxation rates measured upon heating were the same as those measured upon cooling. For CsC_{60}, relaxation measurements were repeated at 30-min intervals at a fixed temperature until three successive measurements yielded the same T_1 value within the experimental error.

No signals attributable to unreacted C_{60} or to A_3C_{60}, A_4C_{60}, or A_6C_{60} compounds were observed in our ^{13}C, ^{133}Cs, and ^{87}Rb NMR spectra. These other phases are therefore present at levels less than 5%, if at all, in our RbC_{60} and CsC_{60} samples.

III. RESULTS

Figures 1 and 2 show ^{133}Cs and ^{13}C NMR spectra of CsC_{60} at various temperatures. Figure 3 shows the temperature dependences of the ^{133}Cs and ^{13}C SLR rates. Figures 4 and 5 show ^{87}Rb and ^{13}C NMR spectra of RbC_{60}. Figure 6 shows the temperature dependences of the ^{87}Rb and ^{13}C SLR rates. The frequency scales for ^{133}Cs, ^{87}Rb, and ^{13}C NMR spectra represent fractional frequency shifts $\Delta\nu/\nu_0$ from 1-M $CsCl_{(aq)}$, 1-M $RbCl_{(aq)}$,

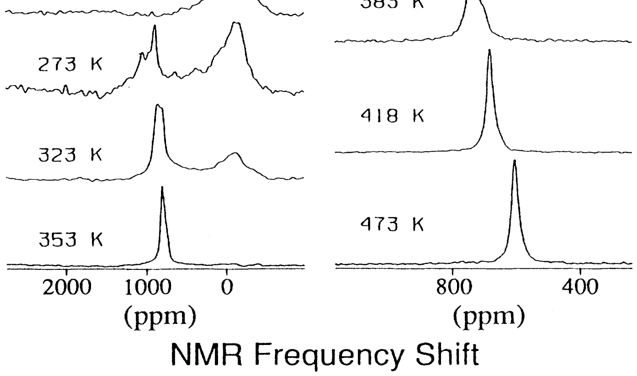

FIG. 1. ^{133}Cs NMR spectra of CsC_{60} at the indicated temperatures. Note the different frequency scales for the left and right panels.

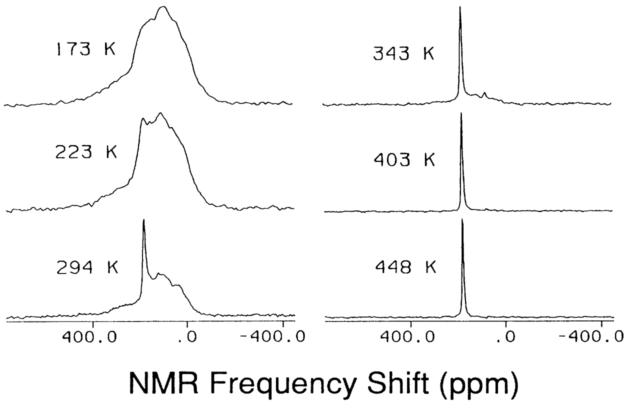

FIG. 2. ^{13}C NMR spectra of CsC_{60} at the indicated temperatures.

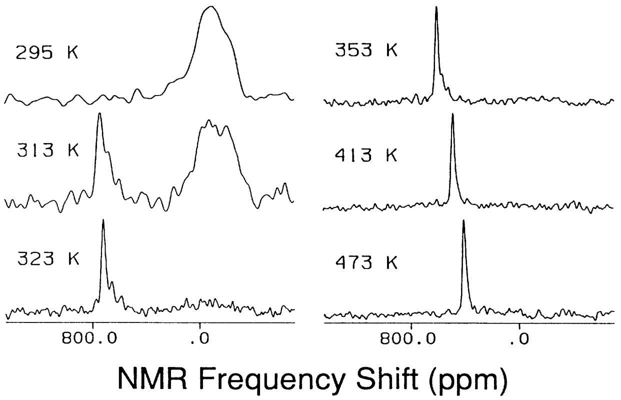

FIG. 4. ^{87}Rb NMR spectra of RbC_{60} at the indicated temperatures.

and tetramethylsilane (TMS) reference signals, respectively, with positive shifts indicating higher resonant frequencies. The reference signals are chosen to be consistent with standard practices but otherwise have no special significance. $^{133}Cs^+$ and $^{87}Rb^+$ in the gas phase resonate near -330 and -210 ppm on the frequency scales in Figs. 1 and 4, respectively.[30]

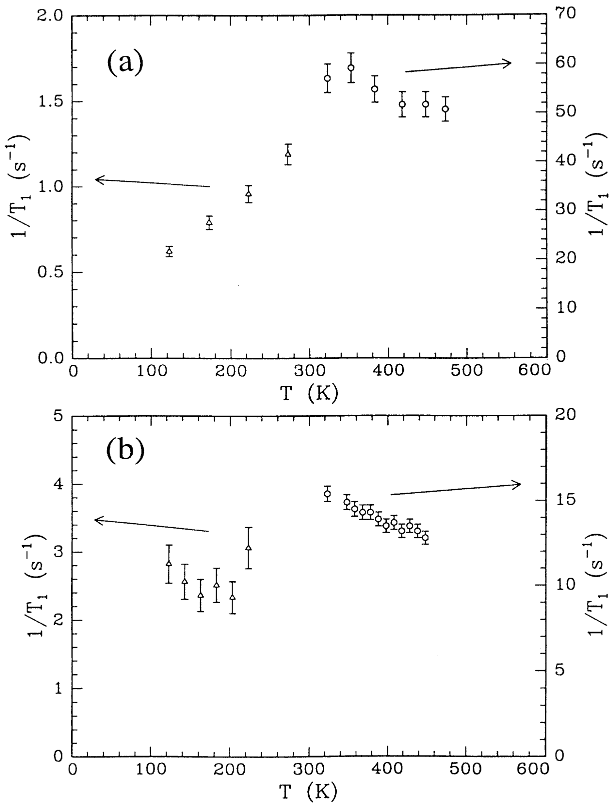

FIG. 3. Temperature dependence of ^{133}Cs (a) and ^{13}C (b) nuclear-spin-lattice relaxation rates in CsC_{60}. Open circles refer to the high-temperature phase; triangles refer to the low-temperature phase. Error bars represent approximate standard deviations, based on the signal-to-noise ratio of the NMR signals.

The NMR spectra clearly show the existence of two phases in both compounds. The LT phase of CsC_{60} gives rise to a broad ^{133}Cs resonance at -200 ppm. The HT phase gives rise to a sharp resonance with a shift that decreases *strongly* with increasing temperature, from 820 ppm at 323 K to 600 ppm at 473 K. Figure 7(a) shows the temperature dependence of the ^{133}Cs NMR shift in the HT phase. In the ^{13}C NMR spectrum of CsC_{60}, the LT phase has a broad resonance with an isotropic shift (center of gravity) of 100 ± 10 ppm. The HT phase has a sharp resonance with a shift that decreases *weakly* with increasing temperature, from 180 ppm at 323 K to 177 ppm at 448 K.

Similarly, the LT phase of RbC_{60} gives rise to a broad ^{87}Rb resonance at -120 ppm. The HT phase gives rise to a sharp resonance with a shift that decreases *strongly* with increasing temperature, from 615 ppm at 353 K to 410 ppm at 473 K. Figure 7(b) shows the temperature dependence of the ^{87}Rb NMR shift in the HT phase. In the ^{13}C spectrum of RbC_{60}, the LT phase has a broad line, while the HT phase has a sharp line with a *weakly* temperature-dependent shift, as in CsC_{60}.

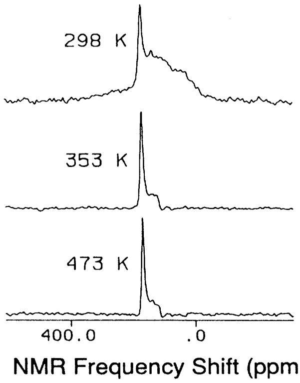

FIG. 5. ^{13}C NMR spectra of RbC_{60} at the indicated temperatures.

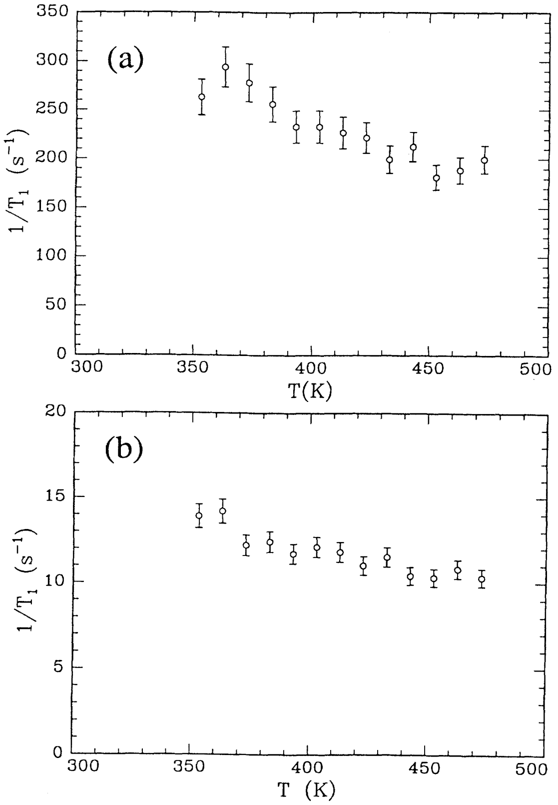

FIG. 6. Temperature dependence of ^{87}Rb (a) and ^{13}C (b) nuclear-spin-lattice relaxation rates in RbC_{60}.

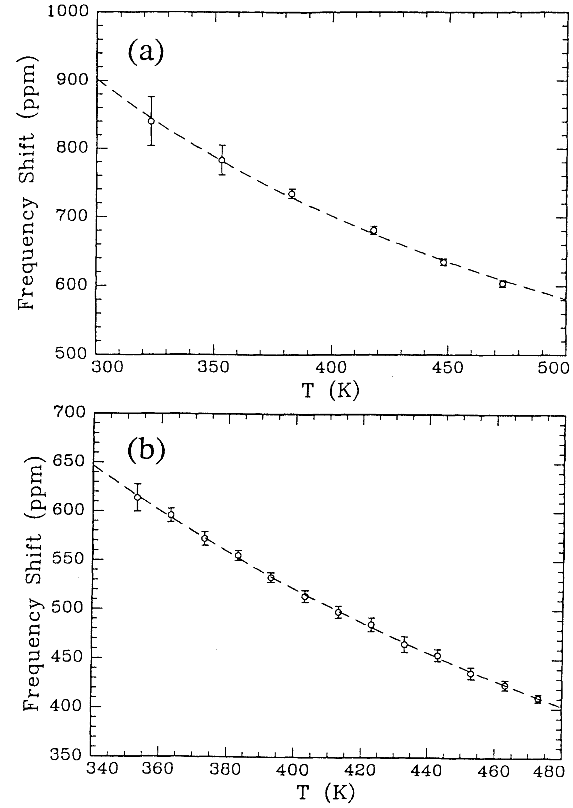

FIG. 7. Temperature dependence of the ^{133}Cs NMR frequency shift in CsC_{60} (a) and the ^{87}Rb NMR frequency shift in RbC_{60} (b). Frequency shifts are measured relative to 1-M $RbCl_{(aq)}$ and 1-M $CsCl_{(aq)}$. Experimental points are for the high-temperature phases of both compounds. Dashed lines are least-squares fits to Curie laws (see text).

In CsC_{60}, NMR signals from the HT and LT phases coexist from about 250 to 350 K. In RbC_{60}, NMR signals from the HT and LT phases coexist from about 295 to 350 K. These coexistence ranges are in rough agreement with those observed in XRD measurements.[26] Differences in the apparent coexistence ranges are attributed to differences in the relative sensitivities of NMR and XRD to the LT and HT phase (e.g., the HT phases are more readily observed in NMR spectra than the LT phases because of the narrower resonance lines) and to possible nonequilibrium phase distributions resulting from rapid temperature changes (i.e., quenching effects).

The small linewidth (5–7 ppm) of the ^{13}C resonance in the HT phases of both compounds indicates that the C_{60}^- ions are rotating isotropically with an orientational correlation time less than 10 μs, as previously observed in pure solid C_{60} (Refs. 31 and 32) and in certain other alkali-metal fullerides.[11,12,23,33] The greatly increased linewidth (250 ppm) in the LT phases indicates that the C_{60}^- ions are static on a time scale of at least 100 μs. The observed ^{13}C shifts in the HT phases (173–175 ppm for RbC_{60}; 177–180 ppm for CsC_{60}) are similar to the ^{13}C shifts in A_2C_{60}, A_3C_{60}, and A_4C_{60} compounds.[11–13,23] The shifts in the LT phases (100±10 ppm) are significantly smaller than any previously observed in alkali-metal fullerides or fullerenes, including pure C_{60} (143 ppm) and the A_6C_{60} compounds (154±5 ppm)[11,23]. The comparatively small ^{13}C shift in the LT phases of RbC_{60} and CsC_{60} may be an important clue regarding the electronic properties of these materials, but it is currently not understood.

The observation of a single sharp line in the ^{87}Rb and ^{133}Cs NMR spectra of the HT phases is consistent with the structures of these phases determined by Zhu *et al.*,[26] in which there is a single type of site occupied by alkali-metal ions, and with rapid rotation of the C_{60}^- ions. The increased ^{87}Rb and ^{133}Cs linewidths in the LT phases may result from the lower crystallographic symmetry, the possible occupation of several inequivalent interstitial sites, the dependence of the alkali-metal shift on the (static and possibly disordered) orientation of neighboring C_{60}^- ions, disorder in the position of the alkali-metal ions within the interstitial sites, or some combination of these factors. ^{133}Cs NMR shifts in $Cs_xRb_{3-x}C_{60}$ have been reported to be −120 and −380 ppm for Cs in tetrahedral and octahedral sites, respectively, at 300 K.[34] We observe ^{87}Rb NMR shifts of 23 and −96 ppm for Rb in the tetrahedral and octahedral sites of Rb_3C_{60}, respectively, at 443 K.[35] Thus the alkali-metal shifts in the LT phases resemble those in A_3C_{60} compounds and are approximately 100 ppm greater than those of the gas-phase ions. The shifts in the HT phases are much larger.

IV. DISCUSSION

A. High-temperature phases, ^{133}Cs and ^{87}Rb NMR

A striking feature of the alkali-metal NMR data in the HT phases of RbC_{60} and CsC_{60} is the large and strongly temperature-dependent shifts. Large but essentially *temperature-independent* shifts (i.e., Knight shifts) might be observed if these phases were metallic and if there were significant conduction-electron probability density at the alkali-metal nuclei (for comparison, the Knight shifts of pure Rb and Cs metals are 6500 and 14 900 ppm, respectively[36,37]). Large and *temperature-dependent* shifts can occur if the excess electrons on C_{60}^{-} ions are primarily localized, i.e., if the HT phases are paramagnets, and if the electron spins fluctuate rapidly due to exchange interactions. We therefore adopt a model for the HT phases of CsC_{60} and RbC_{60} in which the excess electrons act as localized, exchange-coupled paramagnetic centers.

Although the excess electrons are primarily localized on C_{60}^{-} ions, there is a small electron probability density at the alkali-metal nuclei which produces a Fermi contact hyperfine coupling. We assume that each alkali-metal nucleus (in an octahedral site) is coupled equally to electrons on its six nearest-neighbor C_{60}^{-} ions. The temperature-dependent shift of the NMR line then results from the time average of the hyperfine coupling, which is nonzero due to the polarization of the electron spins in the applied dc magnetic field:

$$\frac{\Delta\nu}{\nu_0}=\frac{A_M\sum_{i=1}^{6}\langle S_{zi}(t)\rangle}{\nu_0} \tag{1}$$

$$\approx\frac{3A_M}{2k_BT}\frac{\gamma_e}{\gamma_n}, \tag{2}$$

where S_{zi} is the component of the electron spin of the ith nearest neighbor along the field direction, A_M is the (transferred) Fermi contact hyperfine coupling constant to a single electron spin, and γ_e and γ_n are the gyromagnetic ratios of the electron and the nucleus. Equation (2) assumes that the electron spins are independent of one another and that k_BT is much greater than the electron-spin Zeeman energy (12 K at 9.39 T). The shift then follows a Curie law.

Since the true reference for the ^{87}Rb and ^{133}Cs shifts, which would be the shift in the absence of contact hyperfine couplings or in the infinite-temperature limit, is not known *a priori*, the data in Fig. 7 are fit to the form $\Delta\nu/\nu_0=(b/T)+c$. From these fits, we get $b=(2.85\pm0.15)\times10^5$ ppm-K, $c=-190\pm40$ ppm for ^{87}Rb, and $b=(2.40\pm0.20)\times10^5$ ppm-K, $c=100\pm50$ ppm for ^{133}Cs. The values of b imply $A_M=1.31\times10^{-20}$ erg (1.97 MHz) for ^{87}Rb and $A_M=4.40\times10^{-21}$ erg (0.664 MHz) for ^{133}Cs. For comparison, the hyperfine coupling constants in atomic ^{87}Rb and ^{133}Cs are 4557 and 2627 MHz, respectively.[38] Thus the electron-spin densities at the alkali-metal nuclei in RbC_{60} and CsC_{60} are less than 10^{-3} times the atomic values, supporting the idea that the alkali-metal atoms are almost fully ionized. The excess electrons reside in orbitals with only very small Rb 5*s* or Cs 6*s* character. The values of c derived from the fits in Fig. 7 indicate that the infinite-temperature limit of the ^{87}Rb shift in RbC_{60} is within 60 ppm of the shift of the $^{87}Rb^{+}$ ion in the gas phase, while the infinite-temperature limit of the ^{133}Cs shift in CsC_{60} is 400–500 ppm larger than the shift of the $^{133}Cs^{+}$ ion in the gas phase. The reason for this difference between RbC_{60} and CsC_{60} is not known.

With the assumption that the alkali-metal SLR is driven by the fluctuations of the hyperfine couplings caused by electron-electron exchange couplings, the measurements of the relaxation rates provide an estimate of the strength of the exchange couplings. According to Moriya's treatment of nuclear relaxation in exchange-coupled antiferromagnets and paramagnets,[39] nearest-neighbor exchange couplings lead to a correlation function

$$\langle S_\alpha(0)S_{\alpha'}(t)\rangle=\frac{\delta_{\alpha,\alpha'}}{4}e^{-zJ^2t^2/\hbar^2} \tag{3}$$

for the electron-spin angular momentum components, where J is the exchange coupling constant and z is the number of nearest neighbors, and to a relaxation rate

$$\frac{1}{T_1}=\frac{6A_M^2}{\hbar J}\left[\frac{\pi}{16z}\right]^{1/2} \tag{4}$$

in the "extreme narrowing" ($h\nu_0/J\ll1$) limit. The factor of 6 in Eq. (4) is due to the assumption that six electron spins contribute equally to the alkali-metal SLR. Using $z=12$, appropriate for a fcc lattice, and $T_1=5$ ms, we obtain $J=6.3\times10^{-16}$ erg (3.1 cm^{-1}) for RbC_{60}. Using $z=12$ and $T_1=18$ ms, we obtain $J=2.5\times10^{-16}$ erg (1.3 cm^{-1}) for CsC_{60}. These values of J are small, consistent with the small overlap of the LUMO's of nearest-neighbor C_{60} molecules. The decrease in the ^{87}Rb and ^{133}Cs SLR rates with increasing temperature in the HT phases suggests a corresponding increase in J, as expected if thermal vibrations increase the average overlap. Alternatively, the contact hyperfine couplings may be weakly temperature dependent.

The analysis above assumes that the electron-spin susceptibility follows a simple Curie law over the temperature range of our measurements on the HT phases. The fact that we find $J\ll k_BT$ supports the assumption of a Curie-law susceptibility. Nonetheless, it remains for this assumption to be tested by direct measurements of the susceptibility. Also, one should note that we have not determined the sign of J.

B. High-temperature phases, ^{13}C NMR

For a ^{13}C nucleus coupled to a single electron spin by a contact hyperfine interaction, the analogs of Eqs. (2) and (4) are

$$\frac{\Delta\nu}{\nu_0}\approx\frac{A_c}{4k_BT}\frac{\gamma_e}{\gamma_n}, \tag{5a}$$

$$\frac{1}{T_1}=\frac{A_c^2}{\hbar J}\left[\frac{\pi}{16z}\right]^{1/2}, \tag{5b}$$

where A_C is the (direct) contact hyperfine coupling constant of a ^{13}C nucleus in a $C_{60}{}^-$ ion to an electron spin on the same ion. In the ^{13}C NMR spectra of RbC_{60} and CsC_{60} in the HT phases, we observe a reduction in the shift by approximately 3 ppm from 350 to 450 K. According to Eq. (5a), this implies $A_C \approx 9.9 \times 10^{-22}$ erg (150 kHz). With $J = 4 \times 10^{-16}$ erg, the ^{13}C SLR rate due to the contact hyperfine coupling would then be roughly 0.3 s^{-1}. The experimentally determined ^{13}C SLR rates in the HT phases are much larger [$1/T_1 \approx 13$ s^{-1}; see Figs. 3(b) and 6(b)]. Previously,[11,12] we estimated the contact hyperfine coupling constant in $C_{60}{}^{3-}$ to be roughly 1.1×10^{-20} erg for each electron in the LUMO, based on an unrestricted Hartree-Fock calculation of the ratio of the unpaired electron-spin density at the carbon nuclei in $C_{60}{}^{3-}$ to that in planar $CH_3\cdot$ and on the experimentally measured[40] hyperfine coupling in $CH_3\cdot$. If we assume that $A_C = 1.1 \times 10^{-20}$ erg and $J = 4 \times 10^{-16}$ erg, we obtain $1/T_1 \approx 37$ s^{-1} from Eq. (5b), in reasonable agreement with the experimental values. However, according to Eq. (5a), the ^{13}C shift would then be much more strongly dependent on temperature than observed. Thus, if the value of J determined from our ^{87}Rb and ^{133}Cs NMR measurements is approximately correct, our ^{13}C NMR shift and SLR measurements cannot be explained simultaneously by a Fermi contact hyperfine coupling. A_C is smaller than suggested by our earlier estimate;[11,12] the dominant ^{13}C SLR mechanism in RbC_{60} and CsC_{60} is something other than a Fermi contact hyperfine mechanism.

In pure solid C_{60}, ^{13}C SLR is driven by the molecular orientational dynamics, which couple to the nuclear spins through the anisotropy of the chemical shift.[31,32] This relaxation mechanism leads to a SLR rate that is proportional to the square of the applied static field. We have measured the ^{13}C SLR rates in a 2.37-T field at several temperatures in both RbC_{60} and CsC_{60}. We find these rates to be the same, within experimental error, as those measured in the 9.39-T field [Figs. 3(b) and 6(b)], indicating that the molecular orientational dynamics do not contribute significantly to the measured SLR rates through the shift anisotropy in these compounds.

A likely explanation for the relatively rapid ^{13}C SLR in RbC_{60} and CsC_{60} is provided by the *dipolar* hyperfine coupling. In the context of our model for the HT phases, a dipolar hyperfine coupling would produce a temperature-dependent inhomogeneous *width*, rather than a shift, of the ^{13}C NMR line if the $C_{60}{}^-$ ions were static. The rapid, isotropic rotation of $C_{60}{}^-$ ions would then average out the inhomogeneous dipolar width, resulting in a nearly temperature-independent spectrum as observed. In the following discussion, we estimate the magnitude of the SLR rate that results from the dipolar hyperfine coupling.

In the laboratory frame, the dipolar hyperfine coupling has the form

$$H_d = \frac{3\gamma_e \gamma_n \hbar^2}{r^3} \sum_{m=-2}^{2} (-1)^m T_{-m}(\mathbf{I},\mathbf{S}) Y_m(\theta,\phi) , \tag{6}$$

where $\mathbf{I}$ is the nuclear-spin angular momentum vector operator, $\mathbf{S}$ is the electron-spin angular momentum, and r is the distance between the electron and the nucleus. T_m and Y_m are second-rank irreducible tensor operator components and second-rank spherical harmonic functions, respectively, normalized such that $T_0 = 1/\sqrt{6}(3I_z S_z - \mathbf{I}\cdot\mathbf{S})$ and $Y_0 = 1/\sqrt{6}(3\cos^2\theta - 1)$. If $\psi(\mathbf{r}) = \langle \mathbf{r}|\psi\rangle$ is the wave function for a single unpaired electron on $C_{60}{}^-$ in a molecule-fixed frame, and if the laboratory and molecule-fixed frames are related by a rotation $R(\Omega)$ with Euler angles Ω, then the effective dipolar coupling is

$$\begin{aligned} \langle \psi | R(\Omega)^{-1} H_d R(\Omega) | \psi \rangle \\ &= \left\langle \psi \left| \frac{3\gamma_e \gamma_n \hbar^2}{r^3} \sum_{m,m'} (-1)^m T_{-m} Y_{m'} D_{m'm}(\Omega) \right| \psi \right\rangle & (7) \\ &= 3\gamma_e \gamma_n \hbar^2 \sum_{m,m'} (-1)^m T_{-m} \left\langle \frac{1}{r^3} \right\rangle_{m'} D_{m'm}(\Omega) & (8) \\ &= 3\gamma_e \gamma_n \hbar^2 \sum_{m} (-1)^m T_{-m} d_m(\Omega) , & (9) \end{aligned}$$

where $D_{m'm}(\Omega)$ is a second-rank Wigner rotation matrix element and

$$\left\langle \frac{1}{r^3} \right\rangle_m \equiv \left\langle \psi \left| \frac{1}{r^3} Y_m(\theta,\phi) \right| \psi \right\rangle , \tag{10}$$

$$d_m(\Omega) \equiv \sum_{m'} \left\langle \frac{1}{r^3} \right\rangle_{m'} D_{m'm}(\Omega) . \tag{11}$$

The coefficient of I_+ in the expression on the right side of Eq. (9) is

$$f_+ = 3\gamma_e \gamma_n \hbar^2 \left[\frac{d_0}{2\sqrt{6}} S_- - \frac{d_{-1}}{2} S_z + \frac{d_{-2}}{2} S_+ \right] . \tag{12}$$

At a given orientation of the $C_{60}{}^-$ ion, the SLR rate is proportional to $\langle f_+ f_+^* \rangle$, where the angular brackets denote an average over the electron spin. Using $\langle S_\alpha S_{\alpha'} \rangle = \delta_{\alpha,\alpha'}/4$,

$$\langle f_+ f_+^* \rangle = 9\gamma_e^2 \gamma_n^2 \hbar^4 \left[\frac{|d_0|^2}{48} + \frac{|d_{-1}|^2}{16} + \frac{|d_{-2}|^2}{8} \right] . \tag{13}$$

For isotropically rotating $C_{60}{}^-$ ions, the SLR rate is then, by analogy to Eq. (4),

$$\frac{1}{T_1} = \frac{8\overline{\langle f_+ f_+^* \rangle}}{\hbar J} \left[\frac{\pi}{16z} \right]^{1/2} , \tag{14}$$

where the overbar denotes an average over Ω.

We can estimate the magnitude of the dipolar hyperfine SLR rate in Eq. (14) by assuming that each ^{13}C nucleus is coupled to $\frac{1}{60}$ of an electron in a hydrogenic $2p_z$ orbital centered at that nucleus. Then

$$\psi(\mathbf{r}) = \frac{1}{4} \left[\frac{Z^3}{2\pi a_0{}^3} \right]^{1/2} \left[\frac{1}{60} \right]^{1/2} \frac{Zr}{a_0} e^{-Zr/2a_0} \cos\theta , \tag{15}$$

where Z is the effective nuclear charge. With this choice of $\psi(\mathbf{r})$,

$$\left\langle \frac{1}{r^3} \right\rangle_m = \delta_{m,0} \frac{Z^3}{1800\sqrt{6}a_0^3} , \tag{16}$$

$$\frac{1}{T_1} = \frac{3\gamma_e^2\gamma_n^2\hbar^3}{J} \left\langle \frac{1}{r^3} \right\rangle_0^2 \left[\frac{\pi}{16z} \right]^{1/2} . \tag{17}$$

When screening of the nuclear charge by other electrons is taken into account,[41] the effective charge seen by a $2p$ electron in a *neutral* carbon atom is approximately 3.14. With $J=4\times10^{-16}$ erg, $Z=3.14$, and $z=6$, Eqs. (16) and (17) imply $1/T_1=50\ \mathrm{s}^{-1}$, a factor of 4 *greater* than the experimental values. Good agreement with the experiments is obtained when $Z=2.5$ in Eq. (16). The effective nuclear charge may be somewhat reduced because of the net negative charge on the $C_{60}{}^-$ ion. This calculation shows that the dipolar hyperfine coupling can account for the observed ^{13}C SLR rates within the context of our paramagnetic model for the HT phases of RbC_{60} and CsC_{60} and with exchange couplings on the order of those derived from our analysis of the ^{133}Cs and ^{87}Rb NMR data. Using Eq. (17) and the experimental ^{13}C SLR rates, we can define the average dipolar hyperfine coupling constant to be $A_{\mathrm{dip}} \equiv 3\gamma_e\gamma_n\hbar^2\langle 1/r^3\rangle_0 \approx 1\times10^{-20}$ erg (1.4 MHz).

Recent calculations by Antropov, Gunnarsson, and Liechtenstein[42] show that the ^{13}C SLR in A_3C_{60} compounds may also be dominated by dipolar, rather than contact, hyperfine couplings. The results of the present paper support the conclusions of Antropov, Gunnarsson, and Liechtenstein (see Sec. IV E).

Finally, we point out that the alkali-metal and ^{13}C SLR rates have similar dependences on temperature in the HT phases of RbC_{60} and CsC_{60}. This similarity supports our assumption that the alkali-metal nuclei are relaxed by magnetic interactions with the electron spins, rather than by electric quadrupole interactions (which would not affect the ^{13}C nuclei).

C. Low-temperature phases

The SLR rates of all nuclei are substantially smaller in the LT phases of RbC_{60} and CsC_{60} than in the HT phases (see Fig. 3; the SLR rates in the LT phase of RbC_{60} at 300 K are roughly 1 s^{-1} for ^{13}C and 3 s^{-1} for ^{87}Rb). In addition, all NMR signals shift to lower frequencies in the LT phases. These observations indicate a dramatic change in the electronic properties at the structural phase transition. Specifically, the NMR measurements suggest a large reduction in the electron-spin susceptibility at the transition. One possible mechanism for such a reduction in the susceptibility is the formation of a metallic state. The possibility that the LT phase of CsC_{60} may be metallic is suggested by the ^{133}Cs relaxation measurements, which show a SLR rate that is nearly proportional to T as expected for a normal metal [see Fig. 3(a)]. With $T_1T\approx210$ K s, and assuming that the contact hyperfine coupling for ^{133}Cs nuclei is the same as in the HT phase, we estimate the density of states at the Fermi energy to be $N(E_F)=1/6A_M\sqrt{\hbar/\pi k_BT_1T}\approx7.0\ \mathrm{eV}^{-1}$ per C_{60} molecule, a value comparable to estimates of the density of states in the A_3C_{60} compounds.[11–18] It should be noted, of course, that the value of A_M may be different in the LT phase. Assuming that the LT phase is indeed metallic, the ^{133}Cs Knight shift predicted by the Korringa relation, i.e., in a noninteracting electron model, is $\gamma_e/\gamma_n\sqrt{\hbar/4\pi k_BT_1T}=270$ ppm. It is not possible to compare this prediction directly with the experimental results because of the uncertainty regarding the true reference frequency for ^{133}Cs shifts. The predicted shift is small, however, and is roughly equal to the ^{133}Cs NMR linewidths in the LT phase.

In contrast to the ^{133}Cs relaxation, the ^{13}C SLR rate is practically independent of temperature in the LT phase of CsC_{60} [see Fig. 3(b)]. This is quite unlike the behavior of the HT phase, in which the ^{133}Cs and the ^{13}C SLR rates have similar temperature dependences. The reduction in the ^{13}C SLR rate at the structural phase transition (a factor of 5) is also significantly less than the reduction in the ^{133}Cs SLR rate (a factor of 50). We do not have a definitive explanation for these observations. It appears possible, however, that the ^{13}C relaxation in the LT phase is enhanced by antiferromagnetic spin fluctuations which, because of the structure of CsC_{60}, do not contribute to the net hyperfine fields at the ^{133}Cs nuclei. The NMR relaxation behavior of the LT phase of CsC_{60} is reminiscent of that of the normal state of $YBa_2Cu_3O_7$. In $YBa_2Cu_3O_7$ above T_c, the ^{17}O nuclei in copper-oxide planes have metallic relaxation behavior, while the planar ^{63}Cu nuclei have a nearly temperature-independent SLR rate.[43] This has been explained by a picture in which unpaired electron spins reside on Cu atoms and are coupled antiferromagnetically.[43,44] Antiferromagnetic spin correlations do not affect the ^{17}O relaxation because, by the symmetry of the copper-oxide plane, the net hyperfine field at an ^{17}O nucleus vanishes when the unpaired spins are in an antiferromagnetic configuration. Similarly, unpaired electron spins reside principally on $C_{60}{}^-$ ions in CsC_{60}. If the spins on the nearest-neighbor $C_{60}{}^-$ ions of a given ^{133}Cs nucleus are antiferromagnetically correlated, it is likely that the net hyperfine field at the ^{133}Cs nucleus will be small. The ^{133}Cs SLR rate will then be reduced relative to the ^{13}C SLR rate. The two SLR rates may have different temperature dependences because they may be determined by different spatial components of the electron-spin susceptibility.

A more complete understanding of the electronic properties of the LT phases depends on additional experiments. In particular, extensions of the NMR measurements on CsC_{60} to lower temperatures, additional NMR measurements on the LT phase of RbC_{60}, and further structural characterization of the LT phases are likely to be informative.

D. Comparison with other measurements

^{13}C NMR measurements on KC_{60} indicate a HT phase above 420 K, with properties very similar to the HT phases of RbC_{60} and CsC_{60}, but a phase-separated mixture of $K_{\delta}C_{60}$ ($\delta \ll 1$) and K_3C_{60} below 420 K.[11,27,49] As shown above, we do not observe analogous phase separation in RbC_{60} and CsC_{60}. The possibility that the LT phases are metastable but very long lived cannot be completely eliminated, however.

The proposed paramagnetic state of the HT phases is consistent with the absence of metallic behavior observed in resistivity measurements on thin films.[19,21] The possibility that the LT phases are metallic is not substantiated by resistivity measurements reported to date. On the other hand, electron paramagnetic resonance (EPR) measurements on RbC_{60} (Ref. 45) and CsC_{60} (Ref. 46) show temperature-independent integrated signal intensities below 300 K, consistent with a metallic electronic state in the LT phases. No evidence for superconductivity has been seen in magnetization measurements on RbC_{60} and CsC_{60} down to 4.2 K.[26,47]

E. Comparison with other alkali-metal fullerides

The electronic properties of CsC_{60} and RbC_{60} are strikingly different from those of A_3C_{60} compounds such as K_3C_{60} and Rb_3C_{60}, despite the structural similarities of these materials. It appears that the electronic properties are quite sensitive to the details of the structures, such as the unit-cell dimensions and symmetry, and to the charge state of the $C_{60}{}^{n-}$ ions. This is an intriguing result, since band-structure calculations do not indicate such differences. The factors that account for the different electronic properties are not understood, but the NMR data and analysis presented above should contribute to our understanding.

Differences in the electronic properties of the alkali-metal fullerides show up especially clearly in NMR measurements. In K_3C_{60} and Rb_3C_{60}, the ^{13}C SLR rate has a metallic temperature dependence above T_c, indicative of a Fermi-liquid-like state for the excess electrons on $C_{30}{}^{3-}$ ions.[11–13] The effects of electron-electron interactions are minor.[48] As discussed above, the excess electrons on $C_{60}{}^{-}$ ions in the HT phases of CsC_{60} and RbC_{60} are localized, leading to temperature dependences of the NMR spectra and SLR rates that are characteristic of nuclei interacting with fixed, exchange-coupled paramagnetic centers. Although the fcc lattice parameters of CsC_{60} and RbC_{60} are *smaller* than those of K_3C_{60} and Rb_3C_{60},[6,8,26] localization may be favored in CsC_{60} and RbC_{60} because of the lower density (by nearly a factor of 3) of excess electrons. Apparently, electron-electron interactions play a major role. The A_4C_{60} compounds have not been studied as extensively by NMR. The ^{13}C SLR rate in Rb_4C_{60} increases much more strongly with increasing temperature than expected for a metal (from 0.8 s^{-1} at 120 K to 12 s^{-1} at 350 K), yet the SLR rates are also much greater than expected for a semiconductor or insulator such as Rb_6C_{60}, for which the ^{13}C SLR rate is roughly 0.1 s^{-1} at 300 K. Thus each A_nC_{60} phase exhibits distinctive behavior in NMR measurements.

Previous analyses of ^{13}C SLR measurements on K_3C_{60} and Rb_3C_{60} have assumed that the dominant relaxation mechanism is provided by Fermi contact hyperfine couplings.[11–13] As discussed above, this assumption appears unjustified in light of our ^{13}C NMR measurements on CsC_{60} and RbC_{60} and in light of the calculations of Antropov, Gunnarsson, and Liechtenstein.[42] Instead, dipolar hyperfine couplings dominate. Antropov, Gunnarsson, and Liechtenstein derive an expression for the orientationally averaged ^{13}C SLR rate due to dipolar hyperfine couplings which, in our notation and with the assumption that the orbitals in the conduction band of the A_3C_{60} compounds are constructed from carbon $2p_z$ functions, can be approximated as follows:

$$\frac{1}{T_1} \approx \frac{2\pi\sqrt{6}}{9\hbar} A_{\mathrm{dip}}^2 N(E_F)^2 k_B T \ . \tag{18}$$

In Rb_3C_{60}, $T_1T \approx 100$ K s above T_c. Assuming that the dipolar hyperfine coupling constant is the same as in Sec. IV B ($A_{\mathrm{dip}} \approx 1\times10^{-20}$ erg), Eq. (18) then implies $N(E_F) \approx 34$ eV^{-1} per C_{60} molecule.

The dominance of dipolar hyperfine couplings over contact hyperfine couplings accounts for the anomalously small ^{13}C Knight shifts noted in our previous study of A_3C_{60} compounds.[12] In place of the Knight shifts that would result from contact hyperfine couplings, dipolar hyperfine couplings should produce an inhomogenous broadening of the ^{13}C NMR lines of polycrystalline samples at low temperatures, where the $C_{60}{}^{3-}$ ions are static. The contribution to the NMR linewidth from this dipolar hyperfine broadening is on the order of $(A_{\mathrm{dip}}\sqrt{3/8})(\gamma_e/\gamma_n)N(E_F)$, or roughly 360 ppm with the parameter values derived above. The ^{13}C NMR linewidth (full width at half maximum) in Rb_3C_{60} is in fact 110 ppm above T_c.[12] The large value of $N(E_F)$, which exceeds other estimates for A_3C_{60} compounds,[14–18] and the corresponding overestimate of the ^{13}C NMR linewidth indicate an enhancement of SLR rates in A_3C_{60}.[49]

V. CONCLUSION

NMR spectra and relaxation rates provide clear evidence for the existence of high- and low-temperature phases of RbC_{60} and CsC_{60} with very different electronic properties. The HT phases are paramagnets, with an exchange coupling of roughly 4×10^{-16} erg (2 cm^{-1}) between electron spins localized on $C_{60}{}^{-}$ ions. The ^{87}Rb and ^{133}Cs NMR shifts and spin-lattice relaxation rates are determined by Fermi contact hyperfine couplings to the localized electron spins, with coupling constants of 1.3×10^{-20} erg (2.0 MHz) for ^{87}Rb and 4.4×10^{-21} erg (0.66 MHz) for ^{133}Cs. The ^{13}C SLR rates are determined by dipolar hyperfine couplings of roughly 1×10^{-20} erg (1.4 MHz) to the electron spins. The Fermi contact hyperfine couplings for ^{13}C nuclei are small, roughly 1×10^{-22} erg (150 kHz), and do not contribute significantly to the SLR rates. All NMR shifts and SLR rates are reduced in the LT phases, indicating a substantial reduction in the electron-spin susceptibility at the structural phase transition. The electronic properties of the LT phases are not well understood, but the possibility exists that the LT phases may be metallic, with antiferromagnetic spin fluctuations that enhance the ^{13}C SLR rates but not the alkali-metal SLR rates. These results, in combination with earlier studies, demonstrate the range of electronic properties that are possible within the class of alkali-metal fulleride materials. The electronic properties appear to be strongly affected by the details of the crystal structure (i.e., the lattice parameter, intercalation sites, and symmetry) and by the state of reduction of the C_{60} units (i.e., the stoichiometry).

ACKNOWLEDGMENTS

We thank S. H. Glarum for discussing his unpublished EPR results with us, and A. J. Millis for suggesting the analogy between our NMR results on the LT phase of CsC_{60} and those on $Yba_2Cu_3O_7$. We appreciate helpful discussions with S. E. Barrett throughout the course of this work. We thank M. J. Rosseinsky, M. A. Cichy, W. J. Romanow, R. M. Strongin, and A. B. Smith III for providing the materials used in this study. Work at the University of Pennsylvania was supported by the National Science Foundation MRL program under Grant No. DMR91-20668 and by the Department of Energy, DE-FC02-86ER45254 and DE-FG05-90ER75596.

---

[1] R. C. Haddon *et al.*, Nature **350**, 600 (1991).

[2] A. F. Hebard *et al.*, Nature **350**, 600 (1991).

[3] M. J. Rosseinsky *et al.*, Phys. Rev. Lett. **66**, 2830 (1991).

[4] K. Holczer *et al.*, Science **252**, 1154 (1991).

[5] K. Tanigaki *et al.*, Nature **352**, 222 (1991).

[6] R. M. Fleming *et al.*, Nature **352**, 787 (1991).

[7] R. C. Haddon, J. Am. Chem. Soc. **109**, 1679 (1987); J. M. Hawkins *et al.*, *ibid.* **113**, 7770 (1991).

[8] P. W. Stephens *et al.*, Nature **351**, 632 (1991).

[9] R. M. Fleming *et al.*, Nature **352**, 701 (1991).

[10] O. Zhou *et al.*, Nature **351**, 462 (1991).

[11] R. Tycko *et al.*, Science **253**, 884 (1991).

[12] R. Tycko *et al.*, Phys. Rev. Lett. **68**, 1912 (1992).

[13] W. H. Wong *et al.*, Europhys. Lett. **18**, 79 (1992).

[14] A. P. Ramirez *et al.*, Phys. Rev. Lett. **69**, 1687 (1992).

[15] Y. Isawa *et al.*, Phys. Rev. Lett. **69**, 2284 (1992).

[16] T. Inabe *et al.*, Phys. Rev. Lett. **69**, 3797 (1992).

[17] S. Saito and A. Oshiyama, Phys. Rev. Lett. **66**, 2637 (1991).

[18] S. C. Erwin and W. E. Pickett, Science **254**, 842 (1991).

[19] G. P. Kochanski *et al.*, Science **255**, 184 (1992).

[20] X.-D. Xiange *et al.*, Science **256**, 1190 (1992).

[21] F. Stepniak *et al.*, Phys. Rev. B **48**, 1899 (1993).

[22] R. F. Kiefl *et al.*, Phys. Rev. Lett. **69**, 2005 (1992).

[23] D. W. Murphy *et al.*, J. Phys. Chem. Solids **53**, 1321 (1992).

[24] J. Winter and H. Kuzmany, Solid State Commun. **84**, 935 (1992).

[25] O. Zhou *et al.*, in *Novel Forms of Carbon,* edited by C. L. Renchler, J. J. Pouch, and D. M. Cox, MRS Symposia Proceedings No. 270 (Materials Research Society, Pittsburgh, 1992), p. 191.

[26] Q. Zhu *et al.*, Phys. Rev. B **47**, 13 948 (1993).

[27] D. M. Poirier and J. H. Weaver, Phys. Rev. B **47**, 10 959 (1993).

[28] J. P. McCauley *et al.*, J. Am. Chem. Soc. **113**, 8537 (1991).

[29] E. R. Andrew and D. P. Tunstall, Proc. Phys. Soc. **78**, 1 (1961).

[30] B. Lindmann and S. Forsen, in *NMR and the Periodic Table,* edited by R. K. Harris and B. E. Mann (Academic, New York, 1978).

[31] R. Tycko *et al.*, Phys. Rev. Lett. **67**, 1886 (1991).

[32] R. D. Johnson *et al.*, Science **255**, 1235 (1992).

[33] S. E. Barrett and R. Tycko, Phys. Rev. Lett. **69**, 3754 (1992).

[34] Y. Maniwa *et al.*, Solid State Commun. **82**, 783 (1992).

[35] R. E. Walstedt *et al.*, Nature **362**, 611 (1993).

[36] H. S. Gutowsky and B. R. McGarvey, J. Chem. Phys. **20**, 1472 (1952).

[37] B. R. McGarvey and H. S. Gutowsky, J. Chem. Phys. **21**, 2114 (1953).

[38] P. Kusch and V. W. Hughes, in *Handbuch der Physik,* edited by S. Flugge (Springer-Verlag, Berlin, 1959), Vol. 37, Pt. 1.

[39] T. Moriya, Prog. Theor. Phys. **16**, 23 (1956); **16**, 641 (1956); A. Narath, in *Hyperfine Interactions,* edited by A. J. Freeman and R. B. Frankel (Academic, New York, 1967).

[40] R. W. Fessenden, J. Phys. Chem. **71**, 74 (1967).

[41] E. Clementi and D. L. Raimondi, J. Chem. Phys. **38**, 2686 (1963).

[42] V. P. Antropov *et al.*, Phys. Rev. B **47**, 12 373 (1993).

[43] R. E. Walstedt and W. W. Warren, Jr., Science **248**, 1082 (1990), and references therein.

[44] A. J. Millis, H. Monien, and D. Pines, Phys. Rev. B **42**, 167 (1990).

[45] S. H. Glarum (unpublished). The EPR signal intensity corresponds to $N(E_F) \approx 4.5\ \text{eV}^{-1}$ per C_{60} molecule in RbC_{60}.

[46] Y. Murakami *et al.*, Mater. Sci. Eng. (to be published).

[47] D. W. Murphy, A. P. Ramirez, and R. B. van Dover (unpublished).

[48] G. Quirion *et al.*, Europhys. Lett. **21**, 233 (1993).

[49] R. Tycko, J. Phys. Chem. Solids (to be published).